$[Cu_4\{Se_2P(O^iPr)_2\}_4]$: A Novel Precursor Enabling Preparation of Nonstoichiometric Copper Selenide ($Cu_{2-x}Se$) Nanowires

Yung-Jung Hsu,[†] Chiu-Ming Hung,[‡] Yi-Feng Lin,[†] Ben-Jie Liaw,[‡] Tarlok S. Lobana,[‡] Shih-Yuan Lu,*[,†] and C. W. Liu*[,‡]

Department of Chemical Engineering, National Tsing-Hua University, Hsinchu, Taiwan 30043, Republic of China, and Department of Chemistry, National Dong-Hwa University, Hualien, Taiwan 97401, Republic of China

Received February 27, 2006. Revised Manuscript Received May 12, 2006

A newly synthesized, selenium-bridged copper cluster $[Cu_4\{Se_2P(O^iPr)_2\}_4]$ was employed in a single-source chemical vapor deposition (SSCVD) process to produce single-crystalline nonstoichiometric $Cu_{2-x}Se$ nanowires for the first time. This is the first discrete, chalcogen-bridged copper cluster being used successfully for the fabrication of 1D copper chalcogenide nanostructure. The crystalline structure and chemical composition of the resulting nanowires were examined and confirmed with X-ray diffraction, high-resolution transmission electron microscopy, and energy-dispersive X-ray spectrometry analyses. Relevant characterizations revealed that a thin film of CuSe was first formed on the substrate surface due to the thermal decomposition of $[Cu_4\{Se_2P(O^iPr)_2\}_4]$; subsequently, the $Cu_{2-x}Se$ nanowires were grown on the CuSe thin film through a self-catalytic vapor−liquid−solid (VLS) growth mechanism with the Cu particles generated in-situ acting as the catalyst. The $Cu_{2-x}Se$ nanowires were found to possess a direct band gap absorption at 558 nm and emit excitonic photoluminescence at 575 nm.

Introduction

Because of their unique applications in mesoscopic physics and in fabricating optical, electronic, and magnetic nanosized devices, one-dimensional (1D) nanostructures have gained considerable research attention in recent years.[1] Gas-phase deposition is the most common approach for the preparation of 1D nanostructures such as nanowires.[2] Among all of the gas-phase-based methods, the vapor−liquid−solid (VLS) process is the most successful one for the generation of nanowires with single-crystalline structures and in relatively large quantities.[3] An important aspect of nanoscience research today is to investigate and seize the mild reaction routes for the synthesis of 1D nanostructures. The single-source chemical vapor deposition (SSCVD) process, which can be conducted in a simple hot-wall reactor[4] and involves only the vaporization of precursors followed by decomposition and deposition at moderate temperatures, provides a convenient access. Thus, the judicious choice of the precursor is exceedingly important, considering that those compositional elements of the product can all be supplied by one single compound.

The copper selenide-based nanoparticles, for example, CuSe, Cu_3Se_2, and $Cu_{2-x}Se$, have been successfully produced.[5] Here, nonstoichiometric copper selenide, $Cu_{2-x}Se$, is an extrinsic p-type semiconductor with a direct band gap of 2.2 eV and an indirect band gap of 1.4 eV at $x = 0.2$.[6] The indirect energy gap of $Cu_{2-x}Se$ is well within the ideal band gap range of 1.1−1.7 eV for applications as solar energy materials.[7] It can also be used as the superionic conductor material.[8] Thus, it is conceivable that the availability of $Cu_{2-x}Se$ in the form of nanowires with well-controlled chemical and physical properties may bring in new applications.

There are several metal−organic clusters that have been utilized as the single-source precursor for the formation of thin films[9] and nanoparticles.[10] Among the chalcogen-based clusters, only germanium sulfide/selenide was fabricated in

* Corresponding author. E-mail: sylu@che.nthu.edu.tw (S.-Y.L.); chenwei@mail.ndhu.edu.tw (C.W.L.).
[†] National Tsing-Hua University.
[‡] National Dong-Hwa University.

(1) (a) Hu, J.; Odom, T. W.; Lieber, C. M. *Acc. Chem. Res.* **1999**, *32*, 435. (b) Lieber, C. M. *Sci. Am.* **2001**, *285*, 58. (c) Xia, Y.; Yang, P.; Sun, Y.; Wu, Y.; Mayers, B.; Gates, B.; Yin, Y.; Kim, F.; Yan, H. *Adv. Mater.* **2003**, *15*, 353. (d) Huang, Y.; Duan, X.; Lieber, C. M. *Small* **2005**, *1*, 142.
(2) (a) Hu, J.; Jiang, Y.; Meng, X.; Lee, C.-S.; Lee, S.-T. *Small* **2005**, *1*, 429. (b) Hsu, Y.-J.; Lu, S.-Y. *J. Phys. Chem. B* **2005**, *109*, 4398. (c) Hsu, Y.-J.; Lu, S.-Y. *Appl. Phys. A* **2005**, *81*, 573. (d) Hsu, Y.-J.; Lu, S.-Y.; Lin, Y.-F. *Small* **2006**, *2*, 268. (e) Lin, Y.-F.; Hsu, Y.-J.; Lu, S.-Y.; Kung, S.-C. *Chem. Commun.* **2006**, 2391.
(3) (a) Wagner, R. S.; Ellis, W. C. *Appl. Phys. Lett.* **1964**, *4*, 89. (b) Duan, X.; Lieber, C. M. *Adv. Mater.* **2000**, *12*, 298. (c) Wu, Y.; Yang, P. *J. Am. Chem. Soc.* **2001**, *123*, 3165. (d) Lauhon, L. J.; Gudiksen, M. S.; Wang, D.; Lieber, C. M. *Nature* **2002**, *420*, 57. (e) Hsu, Y.-J.; Lu, S.-Y. *Langmuir* **2004**, *20*, 23. (f) Hsu, Y.-J.; Lu, S.-Y.; Lin, Y.-F. *Adv. Funct. Mater.* **2005**, *15*, 1350.
(4) (a) Hsu, Y.-J.; Lu, S.-Y. *Chem. Commun.* **2004**, 2102. (b) Choi, H. S.; Park, H. *J. Am. Chem. Soc.* **2004**, *126*, 6248. (c) Mathur, S.; Barth, S.; Shen, H.; Pyun, J.-C.; Werner, U. *Small* **2005**, *1*, 713.
(5) (a) Wang, W.; Yan, P.; Liu, F.; Xie, Y.; Geng, Y.; Qian, Y. *J. Mater. Chem.* **1998**, *8*, 2321. (b) Malik, M. A.; O'Brien, P.; Revaprasadu, N. *Adv. Mater.* **1999**, *11*, 1441. (c) Xia, Y.; Zheng, X.; Jiang, X.; Lu, J.; Zhu, L. *Inorg. Chem.* **2002**, *41*, 387.
(6) (a) García, V. M.; Nair, P. K.; Nair, M. T. S. *J. Cryst. Growth* **1999**, *203*, 113. (b) Pejova, B.; Grozdanov, I. *J. Solid State Chem.* **2001**, *158*, 49. (c) Xie, Y.; Zheng, X.; Jiang, X.; Lu, J.; Zhu, L. *Inorg. Chem.* **2002**, *41*, 287. (d) Hamilton, M. A.; Barnes, A. C.; Beck, U.; Buchanan, P.; Howells, W. S. *J. Phys.: Condens. Matter* **2000**, *12*, 9525.
(7) Korzhuev, A. A.; Khim, F. *Obrab. Mater.* **1991**, *3*, 131.
(8) Chen, W. S.; Stewart, J. M.; Mickelsen, R. A. *Appl. Phys. Lett.* **1985**, *46*, 1095.

10.1021/cm060478n CCC: $33.50
Published on Web 06/13/2006

the form of nanowires by using these clusters as the precursors.[11] Liu and co-workers have reported several selenium-centered clusters of Cu^{I}, Ag^{I}, and Zn^{II} using dialkyl diselenophosphates (dsep) with nuclearities ranging from 4 to 11, which involve the rupture of the P−Se bond to generate such clusters.[12] These clusters as well as their sulfur counterparts indeed possess potential in several technological applications[13] and have drawn many biological interests.[14] The clusters of copper were explored to prepare copper selenide-based nanowires in view of the importance as highlighted above, but efforts did not yield the desired products. It was apprehended that a cluster of lower nuclearity without a chalcogen at the center might be a better choice, and thus such a tetranuclear cluster $[Cu_4\{Se_2P(O^iPr)_2\}_4]$, **1**, was designed, synthesized, and employed in this work. In this Article, we report the first example of nonstoichiometric copper selenide ($Cu_{2-x}Se$) nanowires prepared under mild CVD conditions by using cluster **1** as the single-source precursor. To the best of our knowledge, none of the chalcogen-bridged copper clusters[15] has been used successfully in the preparation of 1D nanostructures of copper chalcogenide. However, the Cu_2S nanowires and nanorods were reported to form via the thermolysis of copper−thiolate polymer precursors whose structure indeed was not well characterized.[16] Furthermore, the growth of nanowires was conducted under considerably gentle CVD conditions involving low deposition temperatures (<400 °C) and only reduced system pressure (30 Torr). The formation of nanowires is achieved through a self-catalytic VLS growth mechanism.[17]

Experimental Section

Materials. All chemicals were purchased from commercial sources and used as received. Commercial CH_3CN and C_3H_7OH were distilled from P_4O_{10} and Mg, respectively. Both hexane and diethyl ether were distilled from Na. The ligands $NH_4Se_2P(O^iPr)_2$[12d] and starting compounds $Cu(CH_3CN)_4PF_6$[18] were prepared according to the literature methods.

Synthesis of $[Cu_4\{Se_2P(O^iPr)_2\}_4]$. Diethyl ether (80 mL) was added to a Schlenk flask (100 mL) containing $Cu(CH_3CN)_4PF_6$ (1.63 g, 5.75 mmol) and $NH_4Se_2P(OC_3H_7)_2$ (1.87 g, 5.75 mmol). The solution mixture was stirred for 2 h at 0 °C under a dinitrogen atmosphere, and the color changed to yellow during the reaction period. After filtration, the yellow filtrate was evaporated under vacuum and gave $[Cu_4\{Se_2P(O^iPr)_2\}_4]$, **1**, in 80% yield (1.48 g). Single crystals suitable for X-ray diffraction were grown from Et_2O layered with hexane. Anal. Calcd for $C_{24}H_{56}Cu_4O_8P_4Se_8$: C, 19.45; H, 3.81. Found: C, 19.50; H, 3.89. $^{31}P\{^1H\}$ NMR (121 MHz, $CDCl_3$, 25 °C): $\delta = 69.8$ [s, $J_{PSe} = 651$ Hz, 4P, $P(OR)_2$]. ^1H NMR (300 MHz, $CDCl_3$, 25 °C): $\delta = 1.34$ (d, $J_{HH} = 6$ Hz, 48H, $OCH(CH_3)_2$], 4.9 [m, 8H, $OCH(CH_3)_2$]. $^{77}Se\{^1H\}$ NMR (38 MHz, $CDCl_3$, 25 °C): $\delta = -53.72$ [d, $J_{SeP} = 652$ Hz, 8Se, $Se_2P(OR)_2$]. FAB MS, m/z (m/z_{calcd}): 1176.5 (1175.4) $[M]^+$.

Characterization of Compound 1. The elemental analyses were done using a Perkin-Elmer 2400 CHN analyzer. NMR spectra were recorded with Bruker AC-F200 and Advance-300 Fourier transform spectrometers. The $^{31}P\{^1H\}$ and $^{77}Se\{^1H\}$ NMR spectra were referenced externally against 85% H_3PO_4 ($\delta = 0$ ppm) and PhSeSePh ($\delta = 463$ ppm), respectively. Positive FAB mass spectra were carried out with a VG 70-250S mass spectrometer with nitrobenzyl alcohol as the matrix. Pyrolysis GC−MS experiment was conducted with the gas chromatography (GC) column connected in serial to the mass spectrometer (MS), and before the sample entered the GC column there was a furnace to heat the sample to desired temperatures. Compound **1** was injected into a heated GC injection port (250 °C) of a modified Hewlett-Packard 5890 gas chromatograph equipped with a medium polarity fused silica capillary column (0.25 mm × 30 m). The GC−MS transfer line was held at 250 °C, and the mass spectrometer scanned the molecular weight of the sample from 30 to 500. Single-crystal X-ray diffraction analysis was performed on a Bruker AXS P4 diffractometer at $T = 293$ K and Mo Kα radiation ($\lambda = 0.71073$ Å). The data were collected using the $2\theta-\omega$ scan technique. Data reduction was performed with SAINT,[19] which corrects for Lorentz and polarization effects. An empirical absorption correction (Ψ scans) was applied. The structure were solved by the use of direct methods, and the refinement was performed by the least-squares methods on F^2 with the SHELXL-97 package,[20] incorporated in SHELXTL/PC V5.10.[21] Selected crystal data for compounds **1** are given in Table 1.

Formation of $Cu_{2-x}Se$ Nanowires. The CVD reaction was conducted in a hot-wall tubular quartz reactor under reduced pressure. Amorphous fused silica was used as the substrate for the growth of 1D $Cu_{2-x}Se$ nanostructures. The single-source precursor, **1**, was placed in the quartz boat and heated to 100 °C for generation

(9) (a) Petrella, A. J.; Deng, H.; Roberts, N. K.; Lamb, R. N. *Chem. Mater.* **2002**, *14*, 4339. (b) Hill, M. R.; Jones, A. W.; Russell, J. J.; Roberts, N. K. *J. Mater. Chem.* **2004**, *14*, 3198. (c) Hsu, Y.-J.; Lu, S.-Y. *Langmuir* **2004**, *20*, 194.

(10) (a) Cumberland, S. L.; Hanif, K. M.; Javier, A.; Khitrov, G. A.; Strouse, G. F.; Woessner, S. M.; Yun, C. S. *Chem. Mater.* **2002**, *14*, 1576. (b) Osterloh, F. E.; Hewitt, D. P. *Chem. Commun.* **2003**, 1700. (c) Folch, B.; Larionova, J.; Guari, Y.; Guérin, C.; Mehdi, A.; Reyé, C. *J. Mater. Chem.* **2004**, *14*, 2703.

(11) Nath, M.; Choudhury, A.; Rao, C. N. R. *Chem. Commun.* **2004**, 2698.

(12) (a) Liu, C. W.; Chen, H.-C.; Wang, J.-C.; Keng, T.-C. *Chem. Commun.* **1998**, 1831. (b) Liu, C. W.; Shang, I.-J.; Wang, J.-C.; Keng, T.-C. *Chem. Commun.* **1999**, 995. (c) Liu, C. W.; Hung, C.-M.; Chen, H.-C.; Wang, J.-C.; Keng, T.-C.; Guo, K.-M. *Chem. Commun.* **2000**, 1897. (d) Liu, C. W.; Shang, I.-J.; Hung, C.-M.; Wang, J.-C.; Keng, T.-C. *J. Chem. Soc., Dalton Trans.* **2002**, 1974. (e) Santra, B. K.; Hung, C.-M.; Liaw, B.-J.; Wang, J.-C.; Liu, C. W. *Inorg. Chem.* **2004**, *43*, 7570. (f) Liu, C. W.; Hung, C.-M.; Santra, B. K.; Chu, Y.-H.; Wang, J.-C.; Lin, Z. *Inorg. Chem.* **2004**, *43*, 4306. (g) Liu, C. W.; Lobana, T. S.; Santra, B, K.; Hung, C.-M.; Liu, H.-Y.; Liaw, B.-J.; Wang, J.-C. *Dalton Trans.* **2006**, 560. (h) Liu, C. W.; Shang, I.-J.; Fu, R.-J.; Liaw, B.-J.; Wang, J.-C.; Chang, I.-J. *Inorg. Chem.* **2006**, *45*, 2335.

(13) (a) Barnes, A. M.; Bartle, K. D.; Thibon, V. R. A. *Tribol. Int.* **2001**, *34*, 389. (b) Degroot, M. W.; Corrigan, J. F. *Comprehensive Coordination Chemistry II: From Biology to Nanotechnology, Vol. 7*; Pergamon: Oxford, 2004. (c) O'Brien, P.; Pickett, N. L. *Comprehensive Coordination Chemistry II: From Biology to Nanotechnology, Vol. 9*; Pergamon: Oxford, 2004.

(14) (a) Henkel, G.; Krebs, B. *Chem. Rev.* **2004**, *104*, 801. (b) Gonzalez-Durate, P. *Comprehensive Coordination Chemistry II: From Biology to Nanotechnology, Vol. 8*; Pergamon: Oxford, 2004.

(15) Dehnen, S.; Eichhofer, A.; Fenske, D. *Eur. J. Inorg. Chem.* **2002**, 279.

(16) (a) Chen, L.; Chen, Y.-B.; Wu, L.-M. *J. Am. Chem. Soc.* **2004**, *126*, 16334. (b) Larsen, T. H.; Sigman, M.; Ghezelbash, A.; Doty, R. C.; Korgel, B. A. *J. Am. Chem. Soc.* **2003**, *125*, 5638.

(17) (a) Zhou, S.-M. *Mater. Lett.* **2003**, *57*, 3880. (b) Geng, C.; Jiang, Y.; Yao, Y.; Meng, X.; Zapien, J. A.; Lee, C.-S.; Lifshiz, Y.; Lee, S.-T. *Adv. Funct. Mater.* **2004**, *14*, 589. (c) Han, X.; Wang, G.; Jie, J.; Choy, W. C. H.; Luo, Y.; Yuk, T. I.; Hou, J. G. *J. Phys. Chem. B* **2005**, *109*, 2733.

(18) Kubas, G. J. *Inorg. Synth.* **1979**, *19*, 90.

(19) *SAINT V4.043: Software for the CCD Detector System*; Bruker Analytical X-ray System: Madison, WI, 1995.

(20) Sheldrick, G. M. *SHELXL-97: Program for the Refinement of Crystal Structure*; University of Göttingen: Göttingen, Germany, 1997.

(21) *SHELXL 5.10 (PC version): Program Library for Structure Solution and Molecular Graphics*; Bruker Analytical X-ray System: Madison, WI, 1998.

Table 1. Selected Crystallographic Data for {Cu4[Se2P(OiPr)2]4}

formula	$C_{24}H_{56}Cu_4O_8P_4Se_8$
fw	1482.41
space group	*Pn*
a, Å	11.692(4)
b, Å	18.023(7)
c, Å	11.772(5)
α, deg	90
β, deg	90.71(2)
γ, deg	90
V, Å^3	2480.4(17)
Z	2
ρ_{calcd}, g cm^{-3}	1.985
λ(Mo Kα), Å	0.71073
μ, mm^{-1}	7.726
T, K	293(2)
R1[a]	0.0712
wR2[b]	0.1470

[a] $R1 = \sum||F_o| - |F_c||/\sum|F_o|$. [b] $wR2 = \{\sum[w(F_o^2 - F_c^2)^2]/\sum[w(F_o^2)^2]\}^{1/2}$.

of vapors. The vapors were then introduced into the furnace, whose temperature was set at 360 °C, by N_2. Deposition was run at a carrier gas flow rate of 200 sccm and system pressure of ~30 Torr for 2 h.

Characterization of $Cu_{2-x}Se$ Nanowires. The morphology and dimensions of the products were examined with a field-emission scanning electron microscope (SEM, Hitachi S4700). The crystallographic structure of the products was investigated with X-ray diffraction (XRD, MAC Science MXP18), a transmission electron microscope (TEM, JEOL JEM-2010) operated at 200 keV, and high-resolution TEM (HRTEM, JEOL JEM-400EX) operated at 400 keV. The compositional information was obtained with energy dispersive spectrometry (EDS), an accessory of TEM (JEM-2010). The reported TEM-EDS data were averages of at least three samples. UV−visible absorption spectra were obtained using a Hitachi U-3300 spectrophotometer. For photoluminescence (PL) spectroscopy, a Hitachi F-4500 equipped with a xenon lamp (150 W) was used. The excitation wavelength was set at 370 nm. Both absorption and emission spectra were obtained at room temperature under ambient atmosphere. The solvent used to suspend the products was ethanol.

Results and Discussion

The stoichiometric reaction of $NH_4Se_2P(O^iPr)_2$ with $Cu(CH_3CN)_4PF_6$ in diethyl ether afforded a yellow solution from which a yellow crystalline material of $[Cu_4\{Se_2P(O^iPr)_2\}_4]$, **1**, was isolated in ~80% yield. A single resonance with a set of selenium satellites in the ^{31}P NMR coupled with a doublet in the ^{77}Se NMR suggests all dsep ligands of **1** are equivalent in solution. The positive FAB mass spectrum displays a major band at *m*/*z* 1176.5, which can be formulated as $[Cu_4\{Se_2P(O^iPr)_2\}_3]^+$, the intact cluster with a loss of one dsep ligand. However, the detailed conformation of **1** cannot be realized until the single-crystal X-ray diffraction study.

Compound **1** crystallizes in the monoclinic space group *Pn*, with two molecules in the unit cell. In the crystal structure of **1**, four copper atoms, each located at the vertex of a tetrahedron, are held together with four, face-capped diselenophosphate ligands in a trimetallic triconnective connection pattern[22] to form a tetranuclear unit (Figure 1). Each copper atom in **1** is trigonally coordinated to three selenium atoms from three dsep ligands. Selected bond lengths and angles are given in Table 2. The Cu−Se bond

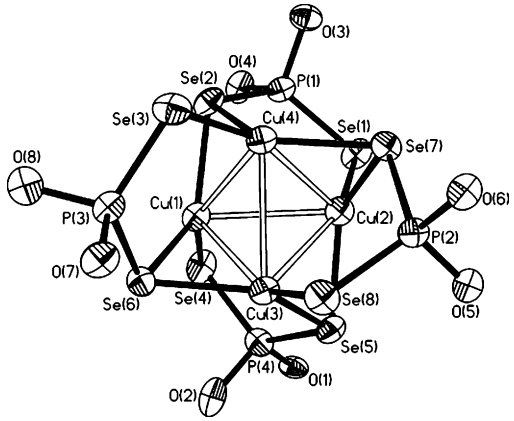

Figure 1. The thermal ellipsoid drawing (50%) of $[Cu_4\{Se_2P(OC_3H_7)_2\}_4]$ with the isopropyl groups omitted for clarity.

Table 2. Selected Bond Distances (Å) and Angles (deg) for Compound 1

Cu(1)−Se(2)	2.354(6)	Cu(4)−Se(3)	2.390(5)
Cu(1)−Se(4)	2.376(5)	Cu(4)−Se(7)	2.362(6)
Cu(1)−Se(6)	2.366(5)	Cu(1)−Cu(4)	2.724(6)
Cu(2)−Se(1)	2.401(5)	Cu(1)−Cu(3)	2.755(6)
Cu(2)−Se(5)	2.379(6)	Cu(2)−Cu(4)	2.711(6)
Cu(2)−Se(7)	2.408(5)	Cu(1)−Cu(2)	2.899(6)
Cu(3)−Se(6)	2.359(5)	Cu(2)−Cu(3)	2.809(6)
Cu(3)−Se(8)	2.387(5)	Cu(3)−Cu(4)	2.875(5)
Cu(3)−Se(5)	2.372(5)	Se−P	2.094(10)−2.217(10)
Cu(4)−Se(2)	2.386(5)		

Cu(4)−Cu(1)−Cu(3)	63.30(14)	Cu(1)−Cu(3)−Cu(4)	57.83(14)
Cu(4)−Cu(1)−Cu(2)	57.55(14)	Cu(2)−Cu(3)−Cu(4)	56.96(15)
Cu(3)−Cu(1)−Cu(2)	59.51(14)	Cu(2)−Cu(4)−Cu(1)	64.47(15)
Cu(4)−Cu(2)−Cu(3)	62.75(14)	Cu(2)−Cu(4)−Cu(3)	60.29(15)
Cu(4)−Cu(2)−Cu(1)	57.98(13)	Cu(1)−Cu(4)−Cu(3)	58.87(14)
Cu(3)−Cu(2)−Cu(1)	57.69(13)	Se−Cu−Se	102.0(2)−129.1(2)
Cu(1)−Cu(3)−Cu(2)	62.79(15)	Se−P−Se	117.5(4)−119.4(4)

lengths are in the range of 2.354(6)−2.408(5) Å, and the angles of Se−Cu−Se average 118.4(2)°. The geometry of the Cu_4 unit is slightly distorted from a regular tetrahedron, which is evident from the angles defined by three adjacent copper atoms ranging from 57.55(14)° to 64.47(15)°. Four out of six edges of the Cu_4 tetrahedron are each bridged by a selenium atom of the dsep ligand, and these Cu−Cu distances ranging from 2.711(6) to 2.809(6) Å are significantly shorter than the other two uncapped Cu−Cu edges, 2.899(6) and 2.875(5) Å. Thus, those Cu−Cu distances that are shorter than the sum of the van der Waals radii for copper (2.80 Å) may be due to the ligand-imposed cluster geometry.[23] Although there are numerous compounds[24] of the Cu_4 tetrahedron surrounded entirely by the sulfur atoms, surprisingly, only two examples, $[Cu_4\{PPh_2(Se)NP(Se)Ph_2\}_3]^+$ and $Cu_4(SePh)_6^{2-}$, having selenium atom shells were reported.[25] Thus, **1** is the first neutral Cu_4 tetrahedron surrounded entirely by the selenium atoms.

The CVD reaction, with cluster **1** as the precursor, was operated at a deposition temperature of 360 °C under nitrogen

(22) Haiduc, I.; Sowerby, D. B.; Lu, S.-F. *Polyhedron* **1995**, *14*, 3389.

(23) Clerac, R.; Cotton, F. A.; Daniels, L. M.; Gu, J.; Murillo, C. A.; Zhou, H. C. *Inorg. Chem.* **2000**, *39*, 4488.

(24) (a) Coucouvanis, D.; Kanodia, S.; Swenson, D.; Chen, S. J.; Stuedemann, T.; Baenziger, N. C.; Pedelty, R.; Chu, M. *J. Am. Chem. Soc.* **1993**, *115*, 11271. (b) Baumgarthar, M.; Schmalle, H.; Dubler, E. *Inorg. Chim. Acta* **1993**, *208*, 135. (c) Liu, C. W.; Staples, R. J.; Fackler, J. P. *Coord. Chem. Rev.* **1998**, *174*, 147. (d) Wyaliff, C.; Bharathi, D. S.; Samuelson, A. G.; Nethaji, M. *Polyhedron* **1999**, *18*, 949. (e) Dai, J.; Munakata, M.; Ohno, Y.; Bian, G.; Suenaga, Y. *Inorg. Chim. Acta* **1999**, *285*, 332.

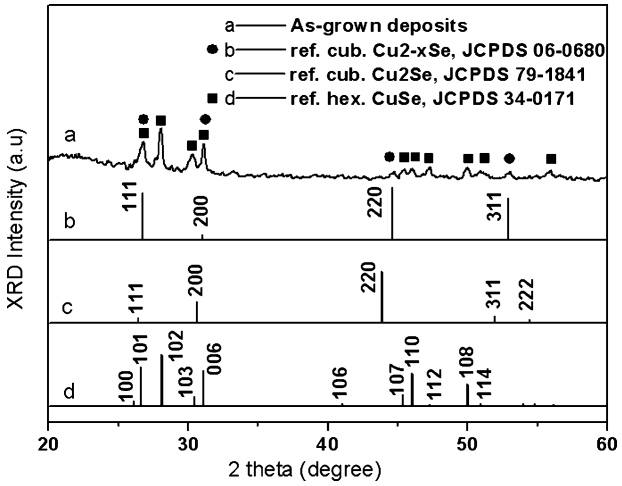

Figure 2. XRD pattern recorded from the as-grown deposits. Also included are three reference XRD patterns for $Cu_{2-x}Se$, Cu_2Se, and CuSe.

atmosphere for 2 h, which yielded black products collected on the surface of fused silica substrates. The XRD pattern of the as-grown samples shown in Figure 2 indicated the formation of both CuSe and $Cu_{2-x}Se$. The presence of cubic $Cu_{2-x}Se$ was revealed by four characteristic diffraction peaks identified from primary reflections at 2θ of 31.06°, corresponding to the (200) plane, and three additional reflections at 2θ of 26.71°, 44.64°, and 52.96° for the (111), (220), and (311) planes, respectively. It may be argued that the above-mentioned diffraction peaks came from the presence of Cu_2Se instead of $Cu_{2-x}Se$. To rule out that possibility, we further examine the diffraction pattern. There are four common crystalline structures for Cu_2Se, monoclinic, orthorhombic, tetragonal, and cubic. The diffraction patterns of the monoclinic, orthorhombic, and tetragonal crystalline structures of Cu_2Se are quite different from that shown in curve a of Figure 2, and thus only the diffraction pattern of cubic Cu_2Se needs to be further considered. The 2θ values of the first three characteristic diffraction peaks of cubic Cu_2Se, corresponding to the (111), (200), and (220) planes, are very close to those of cubic $Cu_{2-x}Se$. Nevertheless, one can differentiate Cu_2Se and $Cu_{2-x}Se$ on the basis of diffraction peaks appearing in the 2θ range of 50−55°. First, there is a 1° difference in 2θ for the (311) plane between the cubic Cu_2Se and cubic $Cu_{2-x}Se$ crystalline structures (51.95° for Cu_2Se and 52.96° for $Cu_{2-x}Se$). From the comparison of patterns a, b, and c of Figure 2 at 2θ around 52°, one can see that the sample contains $Cu_{2-x}Se$ instead of Cu_2Se. Furthermore, for cubic Cu_2Se, there is a diffraction peak at 2θ of 54.447° for the (222) plane, which is not present in curve a of Figure 2. This further supports our conclusion. The XRD pattern also exhibited 10 peaks due to the formation of hexagonal CuSe (two peaks overlap with those of $Cu_{2-x}Se$), which can be identified by comparison with the reference spectrum shown.

SEM observation revealed that the products consisted of a large quantity of nanowires with typical diameter of 30−50 nm and length up to several micrometers, as shown in Figure 3a. Particle heads were consistently present at the tips of the nanowires as shown by the inset arrows of Figure 3b. Also, along the stems of the nanowires, some particle−wire junctions were observed (Figure 3c and d). The nanowires were found to grow accompanied by a thin layer laid on the substrate surface. Figure 3e reveals the morphology of the thin layer, grown with a shorter deposition time of 30 min. Sparsely distributed seedling nanowires were observed on the surface of the thin layer, as indicated by the inset arrows of Figure 3e. This further indicates the growth sequence of CuSe thin film first and $Cu_{2-x}Se$ nanowires later.

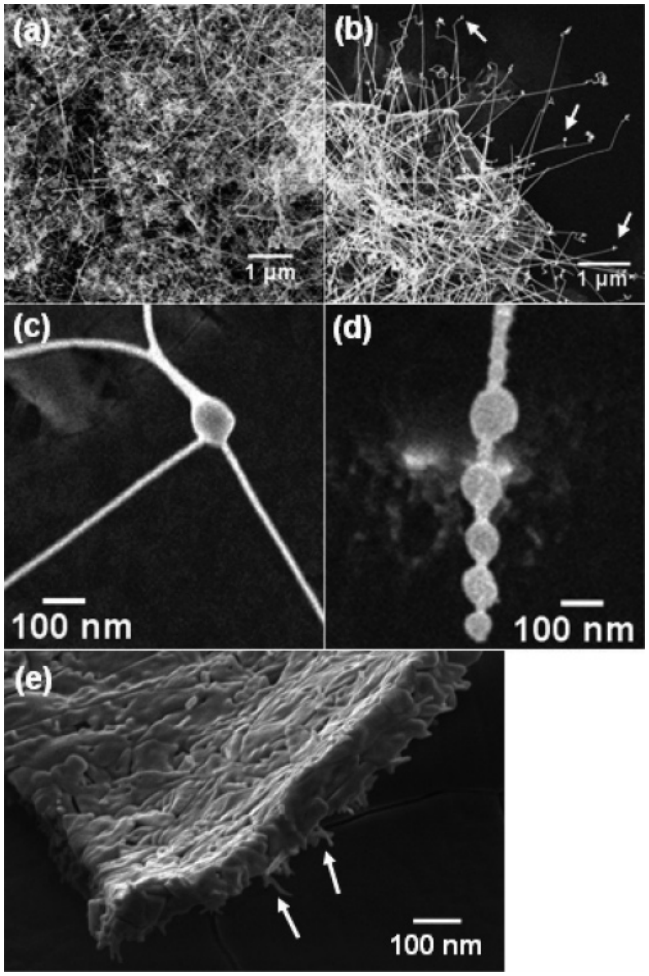

Figure 3. (a,b) Top-view SEM images of the deposits grown on substrates. (c,d) Close-up shots showing the particle−wire−particle junctions. (e) SEM image showing the base thin layer.

A typical TEM image of single free-standing nanowire was shown in Figure 4a. The nanowire imaged here was with a diameter of around 30 nm and possessed a particle at its tip. From the TEM-EDS analyses (Figure 5), the composition of the tip-particle region was rich in Cu with an atomic ratio of 0.85:0.15 for Cu/Se, while the nanowire itself was composed of Cu and Se with an atomic ratio of 0.65:0.35 for Cu/Se. To avoid the misleading Cu signal from the copper grid, nickel grids were used to support the nanowires for the TEM-EDS analysis. The Ni signals in the TEM-EDS analyses of the nanowires (Figure 5) came from the nickel grid on which nanowires were placed. This result, when

(25) (a) Jin, X.; Tang, K.; Long, Y.; Tang, Y. *Acta Crystallogr., Sect. C* **1999**, *55*, 1799. (b) Liu, H.; Banderia, N. A. G.; Calhorda, M. J.; Drew, M. G. B.; Felix, V.; Novosad, J.; de Biani, F. F.; Zanello, P. *J. Organomet. Chem.* **2004**, *689*, 2808.

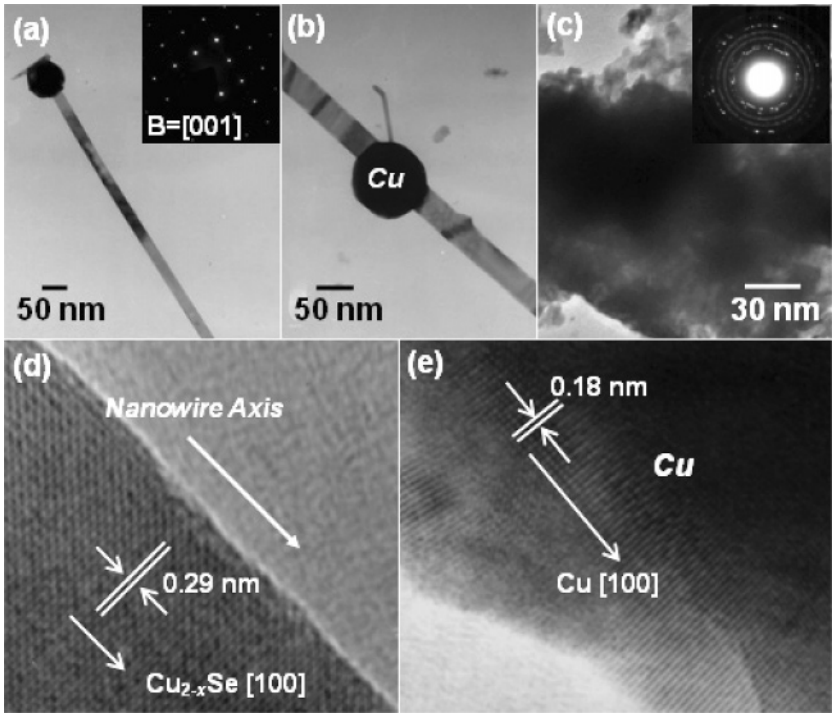

Figure 4. TEM images of the free-standing (a,b) $Cu_{2-x}Se$ nanowires and (c) CuSe thin film, with the corresponding SAED images inset. (d,e) HRTEM images of the stem and tip regions of an individual nanowire, respectively.

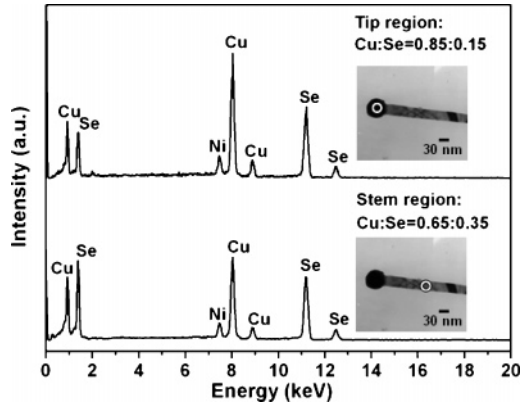

Figure 5. The corresponding TEM-EDS analyses performed at the stem and tip regions of a single nanowire. The Ni signal came from the nickel grid on which nanowires were supported.

combined with that of the XRD analysis, implied that nonstoichiometric $Cu_{2-x}Se$ nanowires were obtained. The dot pattern of the inset selected area electron diffraction (SAED) image showed that the nanowires grew as a single crystal, which can be indexed to the reflection of cubic $Cu_{2-x}Se$ crystals along the [001] zone axis. Figure 4b shows a particle embedded in the stem of a single nanowire. This particle was also found to be rich in Cu according to the corresponding TEM-EDS analysis. The thin film observed at the base of the grown nanowires was also freed with ultrasonic agitation for characterization of its composition. In Figure 4c, the corresponding TEM-EDS analysis shows that the thin film was composed of Cu and Se with an atomic ratio of about 1:1 for Cu/Se. The ring pattern of the inset SAED image can be indexed to the reflection of hexagonal CuSe crystals. The high-resolution TEM image taken at the edge of a single nanowire was displayed in Figure 4d. The lattice image shows an interlayer spacing of 0.29 nm, which agrees well with the lattice spacing of the (200) plane of cubic $Cu_{2-x}Se$ [$d(200) = 0.288$ nm for cubic $Cu_{2-x}Se$, JCPDS file no. of 06-0680]. The axis of the nanowire was found to be parallel to the [100] direction, indicating that the $Cu_{2-x}Se$ nanowire was grown along the [100] direction. The lattice-resolved image of the tip-particle region of the nanowire was shown in Figure 4e. Lattice fringes corresponding to the (200) planes of cubic Cu with a d spacing of 0.18 nm were observed, confirming again that the tip-particle was mainly composed of metal Cu.

On the basis of the results depicted in Figures 2−4, it was envisaged that a thin film of CuSe was first formed on the substrate surface due to the thermal decomposition of **1**; subsequently, the $Cu_{2-x}Se$ nanowires were grown on the CuSe thin film through a self-catalytic VLS growth mechanism with the Cu particles generated in-situ acting as the catalyst (as depicted in Figure 6a). As shown in Figure 1, metal atoms (Cu) are located at the central portion of the precursor molecule with each copper atom being surrounded by three Se atoms. Consequently, CuSe will form first because the Cu−Se bonds already exist. The facile cleavage of the Se−P bond for the dsep ligand in **1** may play a critical role here. In addition, part of Cu^I may undergo disproportionation reactions, leading to the formation of Cu^{II} and metallic copper. While the latter may account for the generation of Cu catalyst to grow $Cu_{2-x}Se$ nanowires, the former could play duel roles in the formation of both CuSe and $Cu_{2-x}Se$. Alternatively, part of Cu^I could be oxidized by free radicals (presumably from isopropoxyl moiety) into Cu^{II} to form CuSe and $Cu_{2-x}Se$. To further prove the validity of the above speculations, **1** was studied by pyrolysis GC−MS (pyrolysis temperature of 250 °C) to develop plausible decomposition pathways/mechanism for the formation of CuSe and $Cu_{2-x}Se$. The result of this study was summarized

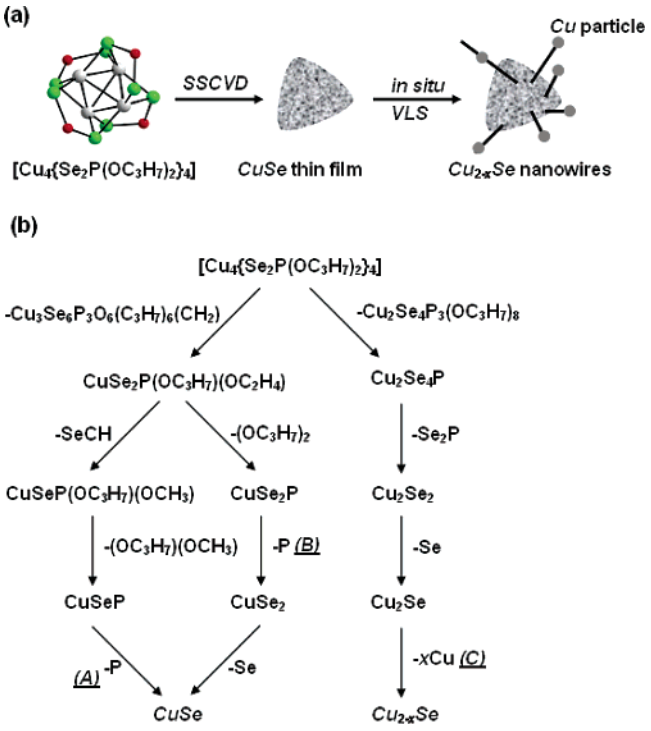

Figure 6. (a) Illustration of the growth mechanism for $Cu_{2-x}Se$ nanowires. (b) Plausible decomposition mechanism for **1** observed from its pyrolysis GC−MS study.

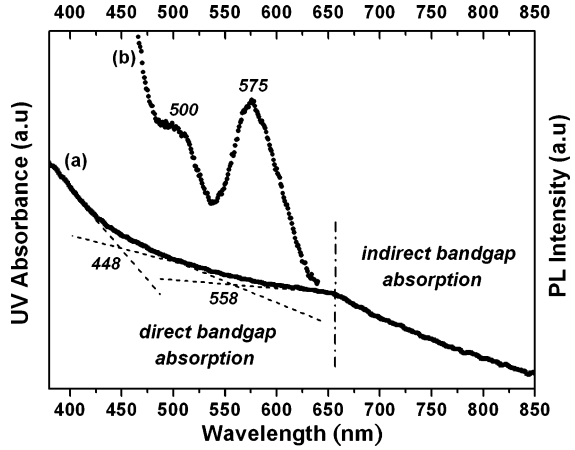

Figure 7. (a) UV−visible absorption and (b) room-temperature PL emission spectra of the product suspended in ethanol. The excitation wavelength for PL measurement was set at 370 nm.

in Figure 6b. The cleavage of Se−P bonds via pathways A and B was responsible for the formation of the CuSe thin film. Additionally, the in-situ generation of metal Cu via pathway C not only supported the suggested Cu-guided self-catalytic mechanism but also accounted for the eventual growth of nonstoichiometric $Cu_{2-x}Se$ nanowires.

The UV−visible absorption spectrum of the product suspended in ethanol was shown as the a-curve of Figure 7. A broad absorption band was observed in the wavelength range of 400−650 nm. The inserted intersecting lines indicate that there are two absorption edges involved in this broad absorption band. $Cu_{2-x}Se$ with $x = 0.2$ was reported to possess a direct band gap of 2.2 eV (absorption wavelength of 564 nm), while there have been reported at least two different direct band gap energies of 2.0 and 2.8 eV for CuSe in the literature (absorption wavelengths of 443 and 620 nm, respectively).[6] The absorption edge at around 558 nm, corresponding to a direct energy band gap of 2.22 eV, was thus attributed to the nonstoichiometric $Cu_{2-x}Se$ nanowires. The absorption edge at around 448 nm (2.77 eV), in good agreement with one of the two reported values for the direct band gap of CuSe, can be attributed to the existence of the first formed CuSe thin film. The two band gap values were close to those reported for $Cu_{2-x}Se$ and CuSe films.[6] Furthermore, the absorption in the wavelength range of 850−650 nm probably came from the indirect band gap absorption of $Cu_{2-x}Se$. The corresponding PL spectrum was shown as the b-curve of Figure 7. An apparent emission band at around 575 nm (2.16 eV) accompanied by a shoulder at 500 nm (2.48 eV) was observed. As compared to the results from the UV−vis spectrum, the predominant emission band at 575 nm was assigned to the excitonic emission of $Cu_{2-x}Se$ via the radiative band-to-band recombination process. As to the minor shoulder at 500 nm, it should come from the defect-related emissions of CuSe, by considering its energy divergence from the observed band gap value in Figure 7a. It should be noted that the trend leading to higher PL intensities for wavelengths shorter than 480 nm was mainly due to the incident excitation beam. In this work, the excitation wavelength was set at 370 nm, and thus the signals near 370 nm in the emission spectrum were strong. In addition, the excitonic emission from the CuSe thin film might also lie in this short-wavelength region and overlap with the scattering of the incident excitation beam.

In this work, the wire−particle junctions were commonly observed in the as-prepared sample. This wire−particle junction has also been observed in other synthetic processes such as self-catalytic VLS[26] and solution−liquid−solid (SLS).[27] A common feature existing in the present work and the above-mentioned examples is that the catalysts were distributed in the growth medium, gaseous or solution, instead of attaching to a substrate. These distributed catalysts in the growth medium can provide the energetically favored sites for adsorption of the targeted materials. Once the product concentration was oversaturated, nanowires of desired materials precipitated out from the catalysts' surfaces. For the typical VLS process with the catalyst particles distributed on the substrate surface, a restricting plane existing at the interface between the catalyst and substrate surface ensures the growth of nanowires only in a specific direction through this restricting plane. As to the present work and the above-mentioned examples, there will be however no restricting planes existing because the catalysts are distributed in the growth medium. As a result, the growth of nanowires could occur in more than one direction on the catalyst surface, and single particles shared by two or more nanowires were observed. In this work, the formation of these wire−particle junctions was common due to the constantly

(26) (a) Chen, Y.; Cui, X.; Zhang, K.; Pan, D.; Zhang, S.; Wang, B.; Hou, J. G. *Chem. Phys. Lett.* **2003**, *369*, 16. (b) Chen, Y. X.; Campbell, L. J.; Zhou, W. L. *J. Cryst. Growth* **2004**, *270*, 505. (c) Chen, Y. Q.; Jiang, J.; Wang, B.; Hou, J. G. *J. Phys. D: Appl. Phys.* **2004**, *37*, 3319.

(27) Trentler, T. J.; Goel, S. C.; Hickman, K. M.; Viano, A. M.; Chiang, M. Y.; Beatty, A. M.; Gibbons, P. C.; Buhro, W. E. *J. Am. Chem. Soc.* **1997**, *119*, 2172.

generated Cu catalyst particles during the decomposition of the precursor.

Conclusions

In conclusion, nonstoichiometric copper selenide $Cu_{2-x}Se$ nanowires were fabricated for the first time, in an SSCVD process by using a newly synthesized tetranuclear, chalcogen-bridged copper cluster $[Cu_4\{Se_2P(O^iPr)_2\}_4]$ as the precursor. The self-catalytic growth of $Cu_{2-x}Se$ nanowires with the Cu particles generated in-situ acting as the catalyst, to the best of our knowledge, was unusual. The facile cleavage of the Se−P bond for the dsep ligand in $[Cu_4\{Se_2P(O^iPr)_2\}_4]$ also played a critical role in the whole decomposition process. The feasibility of using such chalcogen-bridged copper clusters to prepare $Cu_{2-x}Se$ nanowires may open a versatile route to other metal chalcogenide nanostructures.

Acknowledgment. Financial support from the National Science Council of the Republic of China under grants NSC-94-2214-E-007-011 and NSC-94-2113-M-259-010 is gratefully acknowledged.

Supporting Information Available: X-ray data for cluster **1** in CIF format. This material is available free of charge via the Internet at http://pubs.acs.org.

CM060478N